Anthropocene 22 (2018) 20–30

Contents lists available at ScienceDirect

Anthropocene

journal homepage: www.elsevier.com/locate/ancene

Hydrologic impacts of changing land use and climate in the Veneto lowlands of Italy

Anton Pijl[a,*], Claudia C. Brauer[b], Giulia Sofia[a], Adriaan J. Teuling[b], Paolo Tarolli[a]

[a] Dept. of Land, Environment, Agriculture and Forestry, University of Padova, Legnaro, PD, Italy
[b] Hydrology and Quantitative Water Management Group, Wageningen University & Research, Wageningen, Netherlands

ARTICLE INFO

Article history:
Received 26 November 2017
Received in revised form 23 March 2018
Accepted 5 April 2018
Available online 7 April 2018

Keywords:
Land use change
Climate change
Lowland
Urbanisation
Hydrologic modelling
Scenario analysis

ABSTRACT

The Po valley in northern Italy is one of Europe's largest and most anthropogenically-modified lowland areas, where intensifying climate and land transformation are increasingly causing water management problems. In this study, the Wageningen Lowland Runoff Simulator (WALRUS) is calibrated, validated, and applied to a reclaimed basin in the Veneto region (Italy) in order to assess the hydrologic impacts of land use and climate change scenarios. First-time model calibration for Mediterranean lowlands resulted in reasonable performance during the training year (NSE 0.77), but lower validation performance (NSE 0.53), while potential for improved calibration was limited by data availability. Scenario analysis covers the historical and future changes in land cover and climate throughout a century (1951–2060), based on aerial imagery analysis, hydrologic measurements, COSMO-CLM regional climate projections and demographics. WALRUS simulations illustrate how land use transformation (i.e. expanded built-up zones and a diminished drainage network) have a strong potential to increase discharge intensities from the catchment, mostly evident in summer peak flow (past −34%; future +48%). A historical scenario of combined land use and climate shows even stronger deviations from the present (annual discharge −19%; summer peak flow −45%), resulting from an observed increase in rainfall intensity and seasonality over the past 50 years. With drier future climate projections, however, the discharge response is moderate in the combined future scenario. Despite the non-optimal model calibration, the presented work in the Veneto region illustrates the directional impact of processes typical of anthropogenic lowlands. Particularly, the impact of observed land transformation seems to diminish the buffering and storage capacity of the catchment, thereby enhancing the hydrologic risks in modern times.

1. Introduction

Since ancient times, the presence of water has attracted settlements by facilitating agriculture, domestic supply, and transportation, while often favourably located in zones of fertile young soils and minimal elevation differences. Brauer et al. (2014a), based on data by Fan et al. (2013), determined that lowland areas cover over one-fifth of the terrestrial Earth (22%, with groundwater <4 m under the surface), and indeed many of these lowlands are located around densely populated river deltas, coasts, and lakes.

Still, the element of water can be both essential and devastating for the survival of mankind. Increasing flood risk in lowlands can be conceptualised according to Crichton (1999) and Kron (2002) as the combined result of growing *hazard* (e.g. intensifying climate), stronger *exposure* (e.g. growing populations), and more *vulnerability* (e.g. uncontrolled urban sprawl). These trends make our modern societies, in particular in densely populated lowlands, increasingly prone to confrontations with natural forces. In fact, today's massive population size and advanced technologies are affecting planet Earth at an artificial and unprecedented rate and magnitude, which inspires the discussion whether we entered a new anthropogenic epoch: the Anthropocene (Brown et al., 2017; Ellis, 2011; Nature editorial, 2003; Tarolli and Sofia, 2016; Zalasiewicz et al., 2011, 2008).

A major European lowland area where the interplay between man and nature is evident, is the *pianura padana* – or Po valley – in northern Italy. As the nations' longest and largest river basin, the Po catchment consists of fertile plains that were transformed into highly-profitable agricultural lands under favourable climatic conditions. While the area of ~74,000 km^2 covers not even a

* Corresponding author.
E-mail addresses: anton.pijl@phd.unipd.it (A. Pijl), claudia.brauer@wur.nl (C.C. Brauer), giulia.sofia@unipd.it (G. Sofia), ryan.teuling@wur.nl (A.J. Teuling), paolo.tarolli@unipd.it (P. Tarolli).

https://doi.org/10.1016/j.ancene.2018.04.001
2213-3054/

quarter of Italy's total surface, the basin accounts for 40% of the national GDP (Bozzola and Swanson, 2014), indicating the socio-economic momentum of this region. Frequent flood occurrence, however, are causing the loss of lives and high economic damage, which is likely to worsen in the future due to an intensifying hydrologic regime in this region (Dankers and Feyen, 2008) and rapid land use changes. Urbanisation and industrial expansion are common trends in Veneto region (Fabian, 2012; Vaz and Nijkamp, 2015), and are globally known to increase runoff due to surface imperviousness, and to challenge water management due to natural stream development (Chin, 2006; Poff et al., 2006). In parallel, the drainage density of agricultural fields in Veneto has strongly been decreased during the past decades, hence reducing water storage capacity and peak flow buffering (Cazorzi et al., 2013; Sofia et al., 2014). The increasing flood occurrence in this region is partly attributed to these land transformation processes (Pistocchi et al., 2015; Ranzato, 2011; Sofia et al., 2017), and is likely to continue given current demographic trends of growing population, expanding house surface area and diminishing household numbers (ISTAT, 2011; Regione Veneto, 2011a).

In order to quantify these hydrologic impacts under a novel combination of land use and climate scenarios, the novel Wageningen Lowland Runoff Simulator (WALRUS, Brauer et al., 2014a) was applied in a reclaimed coastal basin of the *pianura padana* near Venice. WALRUS is a conceptual hydrologic model specifically developed for lowlands simulations. Due to its high efficiency (in computation and data requirements), open-source structure, and convincing performance, the model is used in water management and research in the Netherlands (e.g. Brauer et al., 2014b) and abroad (e.g. Yan et al., 2016). The hydrogeological conditions of the *pianura padana* polder landscape suggest suitability of the WALRUS model for quantitative scenario analysis in this area. As the model has never been applied in Mediterranean lowlands thus far, this study aims to recalibrate the model, after which it is used to assess the impact of past and future climate and land use trends on hydrological signatures, with special focus on discharge response.

2. Study area

The study area is a 28 km^2 basin along the coast of north-eastern Italy (Fig. 1) in the municipality of Mira (45°26'13.9"N; 12°08'18.3"E). The basin is consists of a typical polder landscape representative for the majority of the Po floodplains (as further shown below): flat, low-lying lands with a dense network of drainage pipes and ditches, which are drained mechanically into the Venice lagoon.

Typical elevations within the study area range between 0 and 2 m AMSL (see Fig. 1B), with depressions exceeding −1 m AMSL in close vicinity to the lagoon, and higher elevations corresponding to artificial river dikes. Such plains of minimal elevation differences are widely spread, with altitudes under 4 m found up to 60 km inland. The slightly elevated portion of the basin drains excessive water directly into the lagoon by elevation differences (Consorzio di Bonifica Acque Risorgive, 2016), whereas the remaining majority depends on mechanical pumping (see Fig. 1A). The area of interest is limited to the latter, defined by the contributing area to the Dogaletto pumping station. There is no natural surface water interaction with the surrounding water bodies, although regulated seasonal inflow occurs to prevent drying (see Section 3.2). Typical groundwater levels of the study area fluctuate between 3 and 0.5 m below the surface, which is representative for the surrounding floodplains (based on seasonal piezometric measurements by Regione Veneto, 2016).

Land use of the study area is dominated by irrigated agriculture (~65%, mainly maize, soy, and wheat), followed by urban and industrial zones (~18%, see Fig. 1C; Regione Veneto, 2007). This land use distribution is homogeneous throughout this zone (e.g. the larger Province of Venice: ~63% irrigated agriculture, ~15% built-up area), where urban zones typically scattered across the countryside are steadily expanding at the cost of cultivated fields (the concept of *città diffusa* described by Fabian, 2012; Vaz and Nijkamp, 2015). A soil inventory by Regione Veneto (2011b) showed that the dominant soil type in the study area is silt loam (~68%, following USDA soil classification), which was used in model calibration. Comparable soil formations are found throughout the floodplains, mostly resulting from river sediments.

3. Materials and methods

3.1. WALRUS model

The large influence of water management actions (such as pumping and surface water control) and the limited amount of hydrological data available for the Veneto region (as shown in the following paragraph) limits the choice of models. WALRUS is the only lumped rainfall-runoff model known to the authors that explicitly accounts for lowland water management practice while requiring little input data. The parametric model was specifically designed for simulations in lowlands, incorporating the primary hydrologic processes and feedbacks characterising such catchments. The open-source model requires few parameters to be calibrated, making it an efficient tool in both event-based analysis and multi-year simulations. The model has never been applied in Mediterranean lowlands before, which resulted in an elaborated calibration procedure for this study. Here follows a concise model introduction with special focus on the model segments affected in this study (Brauer et al., 2014a).

WALRUS is a water balance model based on the conceptualisation of the hydrologic processes of an average cross-section in the catchment (see Fig. 2). Precipitation water (P) is routed to the surface water through the soil (P_V, slow reservoir) or through surface run-off, macro-pore, and drainpipe flow (P_Q, quick reservoir), or by direct impact on the water body (P_S). The soil reservoir consists of a groundwater zone (saturated soil moisture) and a vadose zone (unsaturated, expressed by the storage deficit term d_V). Whereas many models strictly split these zones into separate reservoirs, the groundwater fluctuation within the first meters under the surface (d_G) and interaction with evapotranspiration rates (ET_V) are essential processes in lowlands, and therefore received special attention in the development of WALRUS. Another typical process is the interaction between the groundwater and surface water (f_{GS}) with variable directions (infiltration or drainage) depending on the water management and seasonal levels of both. Artificial surface water levels and mechanical drainage may be the most dominant factors in the hydrologic regime of lowlands. WALRUS incorporates a minimal water level to cause discharge ($h_{S,min}$) and artificial surface water supply or extraction from external sources into its structure (f_{XS}), hence improving the performance and creating potential for water management scenario analyses. The diamond-shaped variables of Fig. 2 relate to the model parameters, which are largely discussed under the calibration section below.

3.2. Model data

WALRUS simulations rely on time series of precipitation, potential evapotranspiration, and external surface water supply. In addition, time series of outlet discharge were used for calibration of the model. For the majority of these variables, data were available from local sources for the calibration period (Section 3.3). However, for the scenario analyses (Section 3.4),

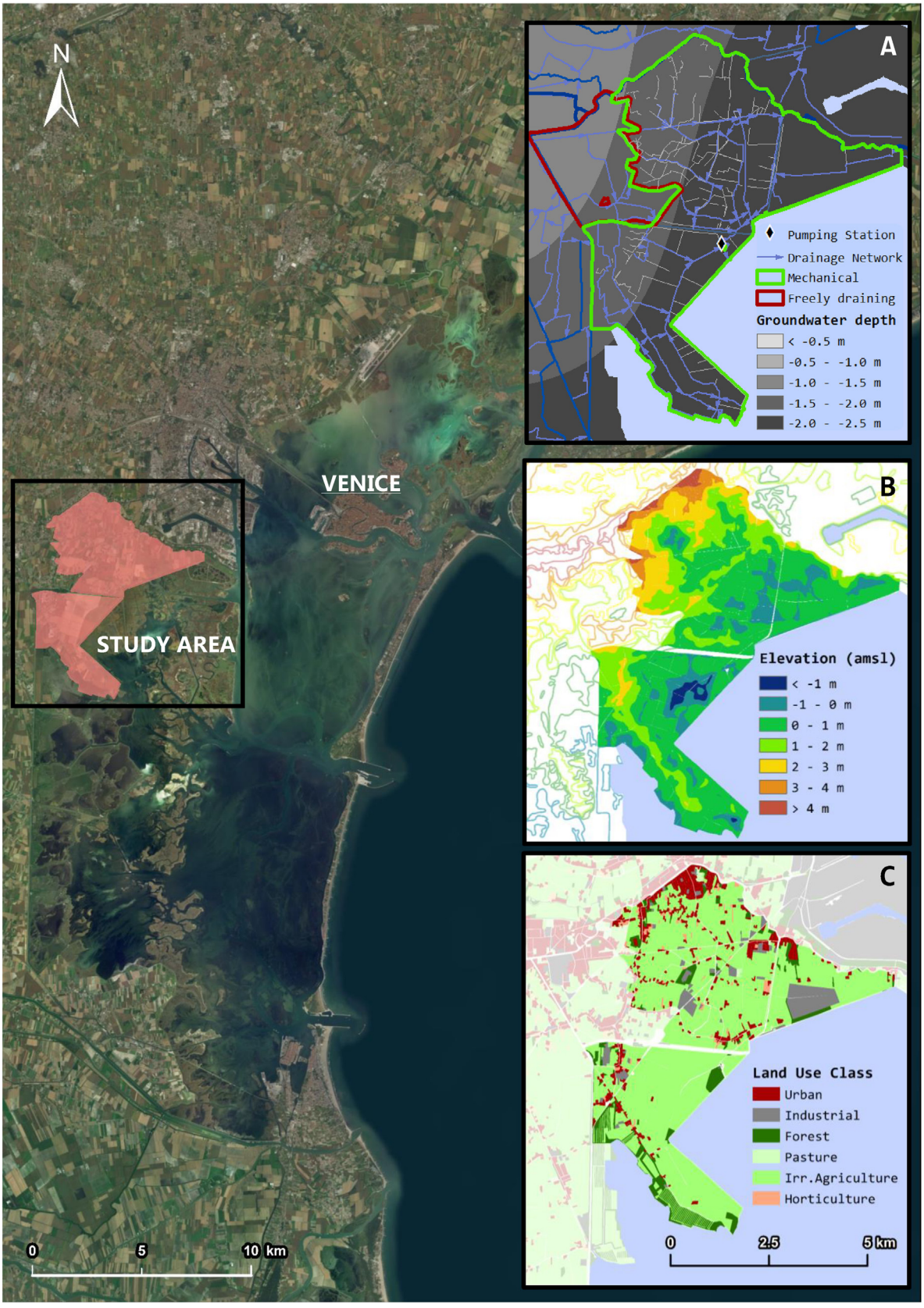

Fig. 1. Location of study area in respect to the Venice lagoon. Inset maps show the drainage system (A), topography (B), and land use classification (C). All maps are work of the author based on data from public web services as referred to in this article.

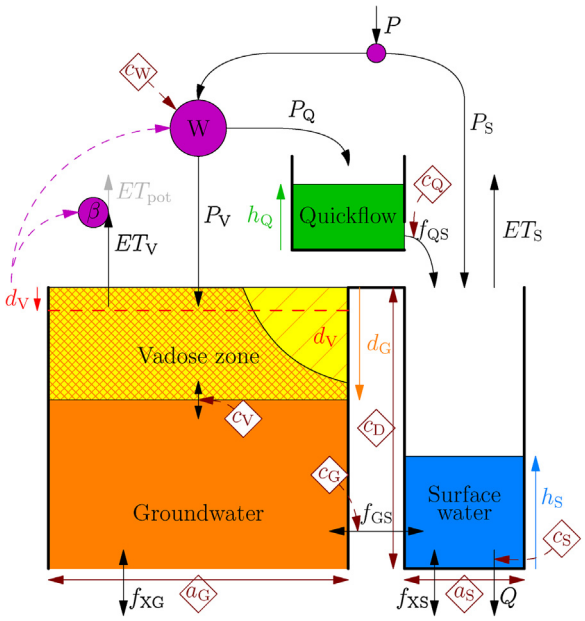

Fig. 2. Overview of WALRUS model structure. Schematic impression of the model reservoirs, fluxes, and parameters as presented by Brauer et al. (2014a).

not all data were covered by historical records and some simplifications had to be made (e.g. evapotranspiration, as discussed in the next paragraphs).

Meteorological data were provided by ARPAV (2016), based on measurements from various stations surrounding the study area. Precipitation records with daily resolution were taken as an average of two surrounding stations at 4–7 km from the study area centroid (inclusion of 9 other surrounding station datasets into the average yielded no noticeable improvements). Precipitation datasets with improved temporal resolution were additionally considered at an earlier stage of the study, but due to the large distance from the study area they were unsuitable (given the local meteorological heterogeneity). Historical climate scenarios were based on another meteorological station with more historical completeness (located in Padova, ~20 km from the study area, 45°23'56.8"N; 11°52'50.7"E), whereas the initial calibration is favoured by the local records of the nearest two stations. The 20-y average precipitation of the surrounding two stations is ~950 mm per annum, with extensive year-to-year variation (e.g. 2011, 2012, 2015 average: 622 mm y^{-1}; while 2010, 2013, 2014 average: 1246 mm y^{-1}).

Reference evapotranspiration data by ARPAV (2016) were available for the period of 2010–2015, which was sufficient for calibration purposes, but limited the scenario implementation. Potential evapotranspiration as input for WALRUS was derived by following the common method by the Food and Agriculture Organization of the United Nations (Smith et al., 1998): crop development stages and related crop coefficients were weighed to the spatial crop occurrence based on Regione Veneto (2007). The resulting crop coefficient series of a typical year was then multipied with reference evapotranspiration rates to derive a potential evapotranspiration time series for this basin. The 2010–2015 average sum is 819 mm per annum, with relatively low year-to-year variation (standard deviation <40 mm).

Discharge rates at the Dogaletto pumping station at the catchment outlet are recorded and provided by Consorzio di Bonifica Acque Risorgive (2016). The actual discharge from the catchment is a combined effect of automated pumping and manual operation by the resident water manager. Discharge time series at daily resolution were provided to serve as calibration and validation datasets, from years 2013 and 2015, respectively. Unfortunately, no more complete discharge records were available from the authorities (data availability is a typical challenge in lowland water management worldwide), which limits the calibration and validation potential, and therefore affects simulation confidence (see more in the discussion section). The annual discharge sums of these two years logically follow precipitation sums closely (1189 mm y^{-1} and 667 mm y^{-1}, resp.).

A series of hydraulic gates allows surface water inflow from the surrounding channel network, in order to provide a source of irrigation water in case the evaporative demand is high during summer. Although precise records of gate operation are missing, the flow capacity is known and typical seasonal inflow was reconstructed by information from Consorzio di Bonifica Acque Risorgive (2016). The missing term in the observed water balance was calibrated, following two principles: (1) the inflow rate is related to the growing season (assuming that supply is proportional to demand); and (2) under rainfall (>1 mm) the hydraulic gates are shut to 20%, regardless of the season. The average addition between 2001 and 2010 equals 552 mm per annum, with strong summer peaks and limited year-to-year variation (standard deviation of 12 mm). Following a similar approach, the extraction of surface water for irrigation purposes is conceptualised following three conditions: (1) no precipitation occurs; (2) evapotranspiration rates exceed 1 mm; and (3) the magnitude is proportional to the evapotranspiration rates (reflecting crop water requirements). The irrigation rates were subtracted from the external surface water supply time series and added to the precipitation series.

3.3. Model calibration

3.3.1. Parameters and modifications

WALRUS was calibrated by setting the Dogaletto catchment characteristics and initial conditions, by modifications to the default model relations, and finally by optimising a set of four calibration parameters.

Catchment characteristics were determined through spatial analysis based on data by Regione Veneto (2011b, 2007) and supported by field observations. The catchment average channel depth was set to 1500 mm, the surface water coverage to 1.6%, and the dominant soil type as "silt loam" (USDA soil class). The initial groundwater depth at 01-01-2013 was set at 750 mm based on seasonal measurements.

Two default model relations were adjusted to the study area. First, the relation between discharge Q and stage height h_S (water level) was adjusted according to discharge observations and known field characteristics. A known minimal water level is maintained (no pumping for $h_s < 0.2$ m), while an exponential function ($y = 0.12e^{6.89x}$) was fitted for $0.2 < h_s < 1.0$ m according to discharge values and a slight extrapolation to approach maximum pumping capacity for this station, for $h_s > 1.0$ m (no such records occurred in the calibration year). The resulting Q-h_S relationship shows a strong discharge response to high water levels, reflecting the observed behaviour. Second, the relation between top soil infiltration (related to the model wetness index W) and soil moisture deficit (d_V) was transformed to mimic the effect of imperviousness area in the land use scenario (Section 3.4.1), as: $W(d_V)_t = a_t + b_t * W(d_V)_{def}$. Here, the wetness index W at period t (*past*, *present* or *future*) has a fixed fractional minimum a_t (the impervious fraction of the study area at time t, resp. 0.032, 0.152, 0.259), while the remaining fraction b_t $(1 - a_t)$ is multiplied by the default function $W(d_V)_{def}$ (described by Brauer et al., 2014a). Thus, the built-up fraction of the study area always leads to the quickflow reservoir, while the remainder depends on the soil wetness.

Four model parameters (wetness index parameter c_W, groundwater reservoir constant c_G, quick-flow reservoir constant c_Q, and vadose zone relaxation time c_V) were optimised for performance and realistic simulations. Analysis of parameter sensitivity and identifiability by the model developers showed that c_W, c_G, and c_Q have the strongest impact and clearest signature on model simulations, of which mostly the former two (for further sensitivity analyses, see Brauer et al., 2014b). Parameter starting values were based on previous studies and physical knowledge of the catchment, and several optimisation methods were applied subsequently. Firstly, a Particle Swarm Optimisation (PSO) algorithm was applied, which is a stochastic population-based technique inspired by the flocking behaviour of birds (Kennedy and Eberhart, 1995). PSO particles (i.e. WALRUS parameter sets) were simultaneously used for an iterative series of model simulations (calibration year-runs) whilst internally communicating their optimisation results (thereby reducing the risk of local minima). A first PSO session involved 20 particles over 20 iterations (using R-package HydroPSO; Zambrano-Bigiarini and Rojas, 2013), which provided new starting values for a second session involving 10 particles over 40 iterations. Additionally, a Levenberg-Marquardt optimisation (dampened least squares method, Marquardt, 1963) of 10 iterations was carried out to confirm the optimum PSO parameter set. The resulting parameter values were slightly adjusted in order to fit the groundwater profile to the seasonal observations (not the primary target variable), giving: $c_W = 27$ mm; $c_V = 15$ h; $c_G = 60 * 10^6$ mm h; $c_Q = 13$ h.

3.3.2. Calibration results and discussion

Model performance was primarily evaluated through a statistical comparison between simulated daily discharge and observed discharge based on the coefficient of determination (NSE) by Nash and Sutcliffe (1970). The NSE of 0.77 for year 2013 (Fig. 4A) reflects reasonable behaviour during the calibration year (ranking mid-high among other WALRUS year-simulations in the country of origin, e.g. Brauer et al., 2014b; De Boer-Euser et al., 2017; Loos, 2015; Slenters, 2014). The validation year 2015 showed worsened performance with a NSE value of 0.53 (Fig. 4B). Anthropogenic processes and management in the basin can partially be held responsible for the non-optimal performance of both years, resulting in simplified model implementations. Furthermore, the strict limitation of two full years of discharge limited the potential understanding of the catchment functioning, especially when considering the extreme annual rainfall of both 2013 and 2015 (resp. 1196 mm and 561 mm, thereby exceeding the standard deviation of 243 mm around the 20-y average of 943 mm).

Goodness-of-fit was additionally determined with the Kling-Gupta Efficiency (KGE, Gupta et al., 2009), and the higher values of 0.88 (2013) and 0.72 (2015) suggest that in part of the simulation inaccuracy may be caused by time shifts not covered by NSE. The deterioration of performance in the validation year could be caused by uncertainty in data or overfitting of the model, although a deeper analysis of performance and sensitivity was not the primary objective of the authors (and was limited by data availability). Nonetheless, simulated discharge response was generally accurate in terms of magnitude and timing (Fig. 4), particularly in the moderate peaks and base flow, while also the relation between the latter and external water supply seems to be balanced. The simulated groundwater profile is close to measurements (Section 2.1), with sharp drops during summer and full recharge towards the end of the year. The disagreement between observed and simulated extreme discharge peaks should be considered in the interpretation of the presented scenario analyses as a source of uncertainty (which is, unfortunately, difficult to resolve due to the strong human factor in the response to extreme rainfall events).

3.4. Scenario analysis

The primary focus of this research is on land use dynamics throughout a century (1951–2060). Secondarily, climate dynamics have been included in the analysis for illustrative purposes. To distinguish the hydrologic impacts of these, different scenarios were conducted along processes and states, including a combined scenario of simultaneous land use and climate change (Table 1). Decadal simulations were conducted at three moments in time: 1951–1960 (*past*); 2001–2010 (*present*); and 2051–2060 (*future*). All quantitative analyses were presented with the present state as a reference for comparing past and future. In the scenario analyses the freely draining north-western part of the basin is included (Fig. 1A), as this reflects the representative land use dynamics better (e.g. the urban sprawl between the cities of Mira and Venice).

3.4.1. Land use scenarios

Land use dynamics in this zone are characterised by a transformation of agricultural fields into impervious urban and industrial zones and the removal of drainage ditches in the rural landscape, reconstructed as follows.

Aerial photographs dating from 1975 were obtained from a public source (IUAV, 2012) and geographically ortorectified to the present land use maps. In the comparison of 1975 imagery and the present-day land use dataset, urban and industrial expansions could be well recognised and quantified. As no observations were available before 1975 and after the present time period, a proxy dataset has been used to extrapolate and reconstruct land use states. In a study of land use change hotspots in Italy, Santini and Valentini (2011) proposed an the following estimation (year-subscript modified to this study):

$$\Delta LU_{1951-1975} = \frac{\Delta LU_{1976-2000} * \Delta POP_{1951-1975}}{\Delta POP_{1976-2000}} \quad (1)$$

where the magnitude of land use change ΔLU (ha) over a simulated period (past or future), is proportional to the population dynamics ΔPOP during that period. In this study we propose a modification to Eq. (1), in order to make land use change a function of total house area *THA* (and underlying demographic trends) instead:

$$\Delta THA = \frac{\Delta POP * \Delta HA}{\Delta HS} \quad (2)$$

where changes in *THA* (ha) are proportional to changes in population numbers ΔPOP and average house areal occupation ΔHA (ha), and inversely proportional to average household size ΔHS. A moderate population projection by the Italian National Institute of Statistics (ISTAT, 2011) was combined with local demographic data on *HA* and *HS* by Regione Veneto (2011a) to compute *THA* for the different time frames. Following the observed historical trends closely, *HA* was assumed to linearly expand whereas *HS* balances out to 2.5 (the last observed point). Finally

Table 1
Overview of simulation scenarios. Land use (L) and climate dynamics (C) were simulated throughout the past (1951–2060; indicated by −), present (2001–2010; indicated by 0) and future (2050+). The combined scenarios of simultaneous land use and climate change are shown diagonally (L_-C_- to L_+C_+). Scenarios depicted in grey are excluded from analysis.

		LAND USE		
		Past	Present	Future
CLIMATE	Past	L_-C_-	L_0C_-	L_+C_-
	Present	L_-C_0	L_0C_0	L_+C_0
	Future	L_-C_+	L_0C_+	L_+C_+

projected land use change was estimated by substituting *POP* for *THA* in Eq. (1) to derive:

$$\Delta LU_{1951-1975} = \frac{\Delta LU_{1976-2000} * \Delta THA_{1951-1975}}{\Delta THA_{1976-2000}} \quad (3)$$

An enhanced land use change projection becomes evident when taking into account the growing areal house occupation and shrinking household sizes (even though *POP* balances out in the moderate scenario). With these projections, the future expansion continues until built-up areas comprise as much as a quarter (26%) of the study area (Fig. 3). These expansions are opposed by a loss of rural areas, primarily those along existing zones and infrastructure (Vaz and Nijkamp, 2015). Given the general vicinity of pasture lands, these were estimated to account for 50% of the loss, while the remaining loss was evenly distributed over the three major crop types (Fig. 3). Note that urban and industrial zones are treated indifferently in this proxy analysis, which can be justified by observed historical expansions.

The consistent ditch removal in the Veneto has been elaborately investigated by Sofia et al. (2014) and Sofia and Tarolli (2017), and their results from similar study areas in close vicinity could be adopted here. Spatial analysis indicates an areal fraction of water of 1.6%, while half a century ago this was double (3.2%). The future estimation was further reduced proportional to the urban expansion (1.43%), assuming that future removal is predominantly caused by replacement with culverts (Ranzato, 2011).

These quantifications led to three modifications to the model set-up for land use scenarios. Firstly, land use transformation has a direct implementation in the W-d_V relation related to surface imperviousness (as discussed in Section 3.3.1). Secondly, a different composition of land classes (Fig. 3) affects the crop coefficient time series and thus evapotranspiration dynamics (and indirectly also the surface water extraction, as discussed in Section 3.2). Thirdly, ditch removal could be directly implemented in the model through the a_S parameter (surface water fraction).

3.4.2. Climate scenarios

Precipitation records for both historical and present scenarios originated from the meteorological station in Padova, thereby preventing interference from spatial variability between the historical and the other scenarios. No historical records of evapotranspiration or light- or temperature proxies were available at any of the stations for inclusion in the climate scenarios; hence the only evapotranspiration changes are the result of land use (i.e. in the transformation to potential evapotranspiration rates). Published trends of the climate model applied in this study (COSMO-CLM, see next paragraph) did not provide a source of historical evapotranspiration changes either, therefore this was left out of the future scenarios in order to allow comparison with historical scenarios. The impact of this simplification is expected to be relatively limited, as motivated in the discussion session.

Future climate analysis in this study consists of a transformed precipitation time series based on the projections by a single regional climate model, serving an illustrative role of potential future climate (while maintaining the focus on scenarios of land use change). Projections under moderate Relative Concentration Pathway 4.5 (Thomson et al., 2011) were based on the COSMO-CLM climate model (Rockel et al., 2008), which has been shown to produce suitable simulations in the lowlands of the Veneto (Bucchignani et al., 2016). Early climate trend analysis here showed inconsistency with findings by other studies, due to comparison between point data (station measurements) and grid data (model simulations). Despite the high spatial resolution of the climate model, with improved simulation skill for extremes (Vautard et al., 2013), a common challenge remains that point-extremes are negated in gridded simulations (Milelli et al., 2008). As statistical downscaling exceeds the scope of this land use-centred study, a transformation of station measurement data was pursued here, following the method by the Royal Netherlands Meteorological Institute (Bakker and Bessembinde, 2012) and based on published COSMO-CLM projections in this region. Firstly, the timeseries was multiplied with monthly anomalies presented by Vezzoli et al. (2015). Secondly, a perturbation on day-scale was carried out, following the impact on precipitation signatures as published by Zollo et al. (2016), i.e. number of rain days, daily intensity, and consecutive wet and dry days. An indirect result of this perturbation under the future climate scenario is introduced by the relation with external surface water supply (Section 3.2).

4. Results

Here the hydrologic impact of different scenarios are discussed, based on WALRUS simulations in the three 10-year timeframes. There is a strong emphasis on the first part, in which the interplay and impact of typical land use change processes are discussed, for these are strongly nested in steady observed trends. Following, the climate change scenario is analysed separately at first, and afterwards in combination with the land use processes.

The numbers and figures presented in this section should be considered in the context of simulation uncertainty discussed in the calibration section. Nonetheless, certain scenarios analyses indicate a clear directional change which agree with known causal

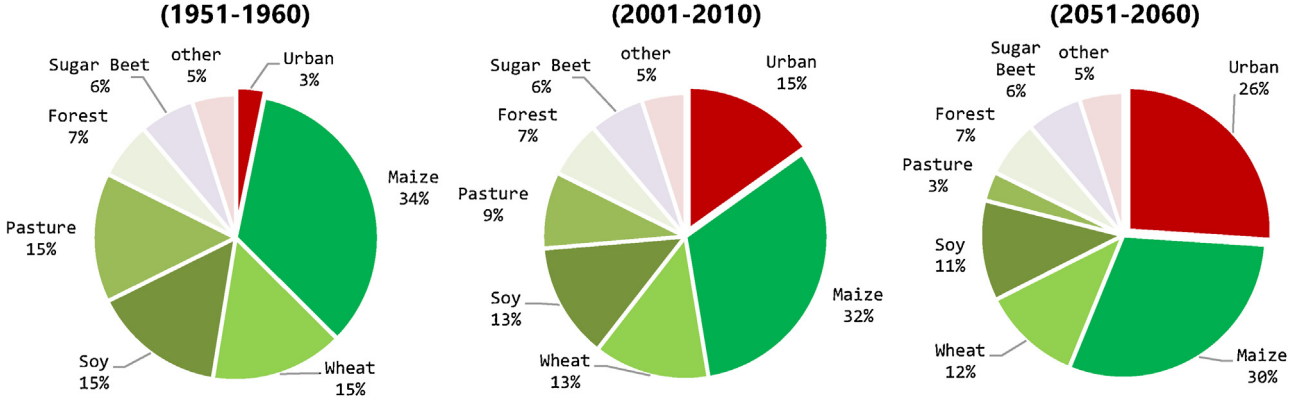

Fig. 3. Land use composition of the study area. A persistent urbanisation trend is projected from the past (A), to the present (B) and future situation (C), at the cost of agricultural fields. The scenarios are reconstructed using spatial analysis of aerial photographs and demographic trend analysis.

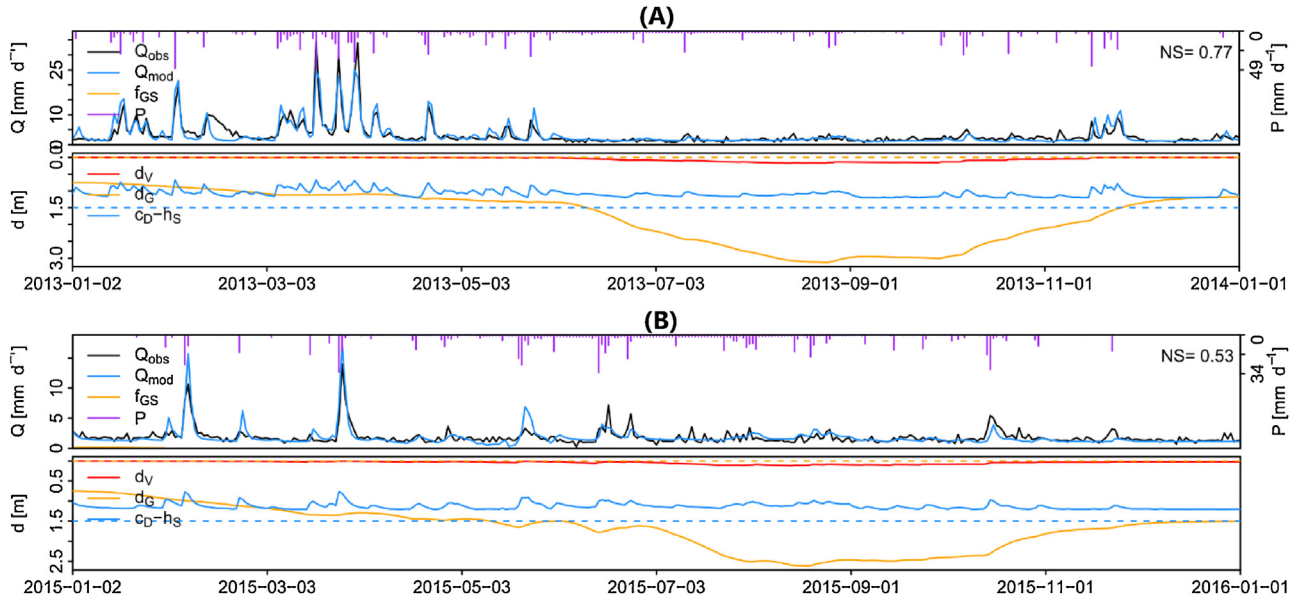

Fig. 4. WALRUS simulations for calibration year 2013 (A) and validation year 2015 (B). The top panels show observed (Q_{obs}, black) vs. simulated (Q_{mod}, blue) discharge and rainfall (purple). Simulated discharge response is generally excellent in timing, although the magnitude shows some error. Fluctuations of groundwater (d_G, yellow) and surface water (c_D-h_S, blue) are displayed in the second panels, in respect to the channel bottom (blue, dashed). The typical groundwater drop during summer is evident, while the surface water levels are artificially maintained through controlled in- and outflow.

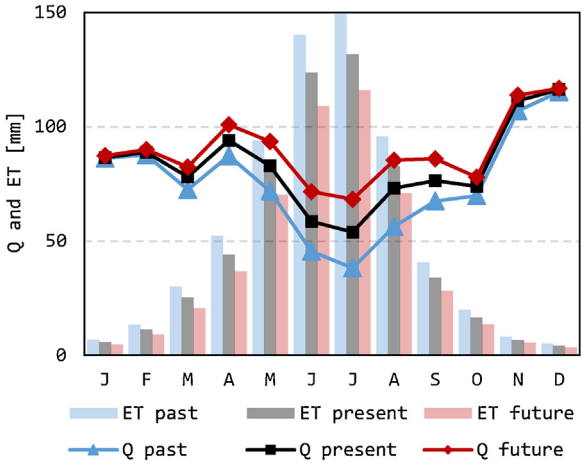

Fig. 5. Monthly evapotranspiration (ET, bars) and discharge (Q, lines). Values are decadal averages under the land use scenarios, showing the typical summer peak. The time spans are depicted in different colours (*past*: 1951–1960; *present:* 2001–2010; *future:* 2051–2060), revealing a progressive reduction of evapotranspiration under the land use scenario.

relationships, and the order of magnitude can be illustrative (although their precise magnitude may be uncertain, as further discussed in the discussion section).

4.1. Impacts under land use scenario

4.1.1. Historical land use processes in detail

The effects of the three land use processes (Section 3.4.1) are analysed individually in a comparison between the present and the past state (50 years). Firstly, evaporative fluxes are progressively limited over time due to the growing simulated fraction of impervious area. This results in an overall positive discharge response, which is accentuated during the summer months due to the seasonal pattern of actual evapotranspiration rates (Fig. 5).

Secondly, the simulated impervious area increasingly limits overall infiltration, causing more quick-flow to occur (e.g. surface runoff, drainage pipes, macro-pores). This process affects the timing and intensity of discharge peaks, responsible for a largely amplified flow regime under present conditions. However, the limited infiltration rates result in a lower groundwater level throughout spring and summer (Table 2). This acts as a buffer of the subsequent autumn storms, thereby moderating peak flow intensity (with similar magnitude to the past scenario).

Table 2
Seasonal analysis under the land use scenarios. Present seasonal values (2001–2010, central column) of discharge (Q), actual evapotranspiration (ET), and groundwater depth (d_G) are accompanied by their relative changes in past (1951–1960) and future (2051–2060). Note that a positive change in d_G corresponds with deeper groundwater.

	LAND USE SCENARIOS											
	L_-C_0				L_0C_0				L_+C_0			
	DJF	MAM	JJA	SON	DJF	MAM	JJA	SON	DJF	MAM	JJA	SON
Sum Q	−1%	−9%	−25%	−7%	291.6	255.0	185.7	261.6 mm	1%	8%	21%	6%
Q_{75}	5%	0%	−18%	−4%	1.3	1.2	1.5	1.3 mm/d	−1%	3%	17%	2%
Q_{20}	−1%	−10%	−27%	−6%	3.7	3.0	2.1	2.4 mm/d	1%	10%	24%	15%
Q_5	−4%	−16%	−34%	−21%	11.3	9.7	3.4	9.9 mm/d	4%	3%	48%	5%
Sum ET	20%	17%	14%	20%	21.1	150.6	338.2	57.3 mm	−18%	−15%	−13%	−18%
Avg. d_G	1%	2%	2%	1%	114.5	136.6	213.8	178.5 cm	−1%	−2%	−2%	−1%
$d_{G,5}$	1%	3%	4%	5%	132.4	161.2	303.9	324.3 cm	−1%	−3%	−4%	−4%

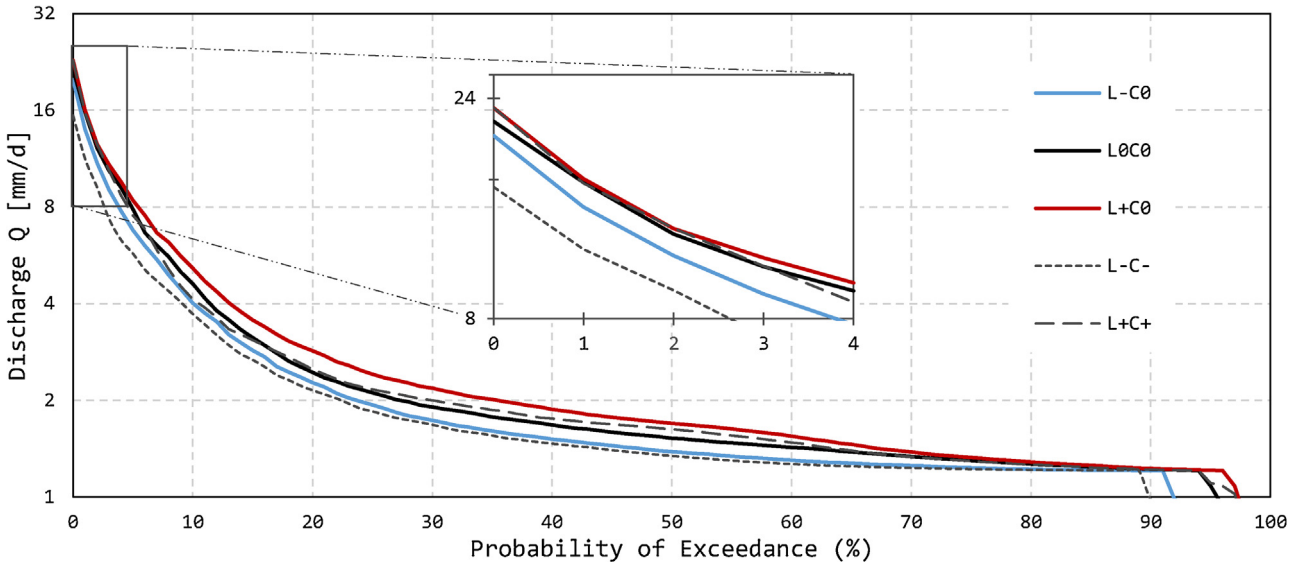

Fig. 6. Flow duration curves under land use (coloured) and combined scenarios (grey, dashed). The distribution of flow intensities is plotted against their probability of exceedance, with an inset of the top 5 peak flow. A progressive flow-inducing effect on the full range is evident under the land use scenarios (coloured lines, L_-C_0 through L_+C_0).

Thirdly, the drainage network is denser in past scenarios, and thus more effective in routing water to the outlet under infiltration-dominated conditions. As channel transport is faster than sub-surface flow, moderate flows are slightly reduced with the present-day drainage network. However, when overland flow is dominant during long or heavy rain storms, this weakening effect becomes less significant. Instead, the reduction of storage capacity in surface water under present conditions results in an increase of the 15% highest discharge.

4.1.2. Flow intensity distribution

The three land use processes combined show an intensifying effect on the full flow range, with −9% annual discharge in the past and +8% in the future. Flow Duration Curves (FDCs, Fig. 6) further show that the historical effect is most apparent in extremes (blue curve), with a 16% reduction in peak flow Q_5 (5% exceedance probability, or 95th percentile discharge; i.e. the ∼182 most severe days of 10 years). Future changes (red curve), instead, amplify mostly the moderate flows (e.g. future Q_{20}: +16%). Furthermore, the highly consistent upward shift of the FDCs highlights the integrity of the presented impacts under the land use change scenario. Incorporation of the climate change scenario and resulting combined scenarios (dashed lines of Fig. 6) are discussed in Sections 4.2 and 4.3 below.

4.1.3. Seasonal impacts

Important intra-annual dynamics are not visible in the flow duration curve analysis – e.g. under the historical scenario, the summer discharge drop (−25%) is much more pronounced than the overall discharge change (−9%). A full quantitative overview of seasonal variation under the land use scenario are presented in Table 2. Actual evapotranspiration rates show a persistent reduction over time resulting from the expanded built-up zones (historical average: +16%, future average: −14%, see also Fig. 5), with the strongest impact on the summer peak. The effect on summer discharge is not only found in base flow but also in peak flow. In fact, historical Q_5 flow during summer was 34% lower than present, stressing the substantial effect of simulated land transformation in the past 50 years. With projected land use change, summer Q_5 flow in the future is simulated to be 48% above present. However, the absolute discharge rates (Table 2, central column) indicate that a strong relative increase does not always point towards the biggest absolute increment. The significance of summer discharge in a year is mostly found in base flow, while demands from the mechanical drainage system are determined by the highest absolute flow rates of the year, typically found in autumn and winter. Potential pumping challenges are therefore likely caused by the +4% and +5% peak flow in the wet seasons (Q_5, DJF and SON, respectively), under the land use scenario.

The simulated groundwater depth shows similar response as the discharge. On average, groundwater tables vary between 1 and 2 m depth, with the deepest groundwater tables occurring in JJA. During dry years, groundwater tables drop to around 3 m (see also Fig. 4). The past land use scenario results in slightly shallower groundwater tables, while the future land use results in deeper groundwater tables for all seasons. The relative deviations are smaller than those for discharge, corresponding to absolute changes of 1 cm in winter to 12 cm in summer and autumn for the 5 percent deepest groundwater tables ($d_{G,5}$).

4.2. Impacts under climate scenario

Meteorological records show a 10% increase in annual precipitation sums over the past 50 years, while future projections indicate a 7% decrease in annual precipitation. These numbers are closely followed by annual discharge simulations in the climate scenario (Table 3). Despite the future reduction, the projected seasonality is more pronounced with drier summers (JJA: −33%) and wetter autumns (SON: +13%; see coloured bars in Fig. 7).

Similar seasonal changes are found in the intensity of rainfall, here expressed by the Simple Daily Intensity Index (SDII, defined

Table 3
As Table 2, but for annual values of all scenarios, i.e. land use and climate scenarios both individual and combined over all time frames.

	ALL SCENARIOS						
	L_-C_-	L_0C_-	L_-C_0	L_0C_0	L_+C_0	L_0C_+	L_+C_+
Sum Q	−19%	−10%	−9%	993.8 mm	8%	−7%	1%
Q_{75}	−6%	0%	−5%	1.3 mm/d	2%	−2%	0%
Q_{20}	−13%	−5%	−7%	2.5 mm/d	16%	−15%	3%
Q_5	−31%	−19%	−18%	9.2 mm/d	4%	−10%	−5%
Sum ET	16%	0%	16%	567.3 mm	−14%	0%	−14%
Avg. d_G	5%	4%	2%	161.1 cm	−2%	9%	7%
$d_{G,5}$	1%	−3%	4%	283.2 cm	−4%	10%	6%

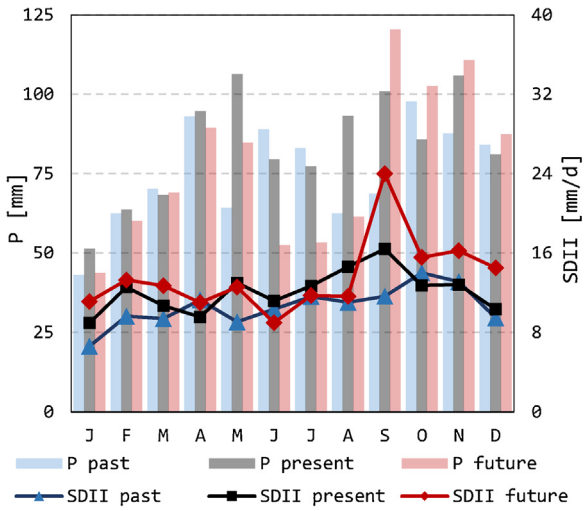

Fig. 7. Monthly precipitation (P, bars) and intensity (SDII, lines), based on decadal averages. The three time spans are depicted in different colours (*past*: 1951–1960; *present:* 2001–2010; *future:* 2051–2060), showing a projected decline of summer rainfall, followed by an increase during autumn and early winter.

by the World Meteorological Organisation as precipitation sum divided by rain days of >1 mm). Throughout the century, SDII values (Fig. 7, lines) show an increase in autumn (SON: past −5%; future +30%) and winter (DJF: past −17%; future +25%). In the future, this trend is again opposed by SDII values of −16% in summer (JJA). Future peak discharge (Q_5) follows this trend, with 32% lower flow intensities in summer and 10% higher flow intensities in winter, according to the climate scenario. This indicates that not only seasonal rainfall sums are diverging, but also its intensity is expected to change accordingly.

4.3. Impacts under combined scenario

Summing up the effects of land use and climate change on seasonal discharge, the historical scenario is the most straightforward (Table 3, see also short-dashed line in Fig. 6). Land use and climate effects are amplified, resulting in a strongly suppressed historical discharge of overall −19%, with a pronounced peak flow reduction (Q_5) of −31%, evident in all seasons (ranging between −45 and −24%). Note that evapotranspiration changes are the sole effect of land use transformation in this scenario analysis (the lacking climate aspect is discussed in Section 5). The past combined scenarios deserves particular attention, as this poses the most realistic and most certain state of comparison with the present (due to historical completeness of observed trends and data).

The future scenario is a mixture of a flow-inducing land use projection and a flow-reducing climate projection (Table 3, long-dashed line Fig. 6), with a slightly induced moderate flow (e.g. Q_{50}: +6%) but peak flow reduction (Q_5: −5%). Furthermore, many seasonal effects are negated (compare Table 2 and Fig. 7), resulting in limited peak flow differences between summer (Q_5: −3%) and winter (Q_5: +10%). Due to the summer drying, groundwater levels drop about 10%, both considering the average level and the extremes of low groundwater.

5. Discussion

The presented results include severe and consistent hydrologic responses (e.g. peak flow) to 100 years of changing land use and climate, although these should be considered in the context of a wide set of uncertainties related to hydrologic modelling (Melsen et al., 2018). Two major types of uncertainty are recognised: the first is related to the understanding of the catchment processes (i.e. model parameterisation), and the second is related to the scenario designs (i.e. perturbations and model implementations).

Model calibration here reflects a general challenge of artificial basins, such as the majority of lowlands worldwide, where the training of a model can become 'mimicking anthropogenic actions'. Although WALRUS can incorporate such fluxes (as done for e.g. external water management, adjusted stage-discharge relationship), records are often missing and behaviour can be subjective and unpredictable. This affected model performance, while the limited length of the datasets (2 years) adds to this uncertainty and involves the risk of overfitting to the calibration dataset. Another uncertainty factor in the parameterisation is the c_G parameter (soil resistance to flow), which should slightly respond to drainage density. Marginal changes in such parameters are hard to quantify with field data and therefore we focussed on the most evident changes. Lastly, the role of initial conditions (e.g. summer groundwater level) in the hydrologic propagation (e.g. autumn discharge and flood risk) can be substantial in lowlands, as also illustrated by Brauer et al. (2016) and Sofia and Tarolli (2017).

Scenario reconstruction and its implementation are unavoidably nested in strong simplifications and assumptions. Firstly, limited by data availability, the reference evapotranspiration profile was fixed for all scenarios. As a result, this work merely shows an evapotranspiration reduction due to land use transformation, which can be considered the upper bound of full expected change. Including climatic evapotranspiration changes would likely enhance the summer drying effect already simulated (Desiato et al., 2015; Milano, 2010; Navarra and Tubiana, 2013), resulting in lower groundwater levels and potentially affecting agricultural production (Boling et al., 2007). However, as pointed out by Sheffield et al. (2012), the impact of evapotranspiration changes on hydrologic extremes is likely to be less direct and severe than the precipitation forcing (while the indirect impact, i.e. a coupling with precipitation, is included in this study), but can depend on the choice of method to calculate reference evapotranspiration. Secondly, a moderate pathway was pursued in the projections of demographics and climate. Thirdly, a single climate model was used for future precipitation forcing, further adding to the intrinsic uncertainty of climate modelling. Nonetheless, the perturbation performed here is largely in agreement with other local model projections (Coppola and Giorgi, 2010; Desiato et al., 2015; Giorgi and Lionello, 2008; IPCC, 2014). Additionally, the simulated impact of climate change on the seasonal discharge profile resembles other hydrologic simulations in the *pianura padana*., e.g. by Vezzoli et al. (2015) on the entire Po discharge, by Coppola et al. (2014) in the upper segment of the Po, and by Baruffi et al. (2012) in two Veneto and adjacent Friuli basins (although the magnitude is subject to simulations period and location).

Still, the utility of the WALRUS model and its application are recognised as well. In an integrated study such as presented, simplifications must be made and the model proved to be efficient in terms of computations (e.g. favouring hundreds of optimisation runs and decadal scenarios) and data requirements (often limited in complex artificial basins). Although a systematic inaccuracy is indicated by non-optimal objective functions, the direction and magnitude of the presented changes are considered important indications of hydrologic impacts. A similar methodology could be useful in e.g. estimating the impact of an expansion of the Dogaletto drainage area (while comparing its maximum capacity), which is currently under consideration for the freely draining zone in Fig. 1A (Consorzio di Bonifica Acque Risorgive, 2016). Another example could be a study of potential summer droughts related to a climate scenario, while comparing the known limitations to external inflow and irrigation practices (and taking into account

the complex drought propagation in anthropogenic basins, Van Loon et al., 2016).

Of particular interest is the comparison between the historical and present scenarios, which is strongly based on observations and trends. The presented impacts on the full flow range, including the most extreme discharge, are convincing in terms of magnitude and sign. The safety and functioning of the basin can thus be challenged as a result of impervious surfaces and a diminished drainage network. The drier future climate scenario partly reverts this land use impact, however, it would be ignorant to use these findings in defence of the business-as-usual scenario of rural transformation. Instead, water management and landscape planning should aim to mitigate these challenges rather than worsening them. The uncertainties related to the future climate and the strong inter-annual variation of this zone furthermore emphasise the importance of resilient hydrologic functioning of the basin (Fatichi et al., 2014), with a focus on local storage capacity and buffering of extremes.

6. Conclusions

The Wageningen Lowland Runoff Simulator (WALRUS) was calibrated in a reclaimed lowland basin in the eastern Veneto region (Italy). Limited availability of training data and uncertainties related to artificial hydrological processes resulted in diminished validation performance (NSE 0.53, KGE 0.72) compared to the convincing calibration results (NSE 0.77, KGE 0.88). Still, model simulations are deemed useful to indicate impacts under scenarios of changing land use and climate (1951–2060), although the precise magnitude should be considered in the context of uncertainty. Land use scenarios were reconstructed based on aerial imagery, spatial analysis and demographic projections. In this scenario, increased soil imperviousness and a diminished drainage network result in growing annual discharge (−9% in the past; +8% in the future), mostly during summer (−25% past; +21% future) and particularly summer peak flow (−34%, past; +48%, future). This indicates an increased demand from the existing drainage system in terms of storage and discharge, also during autumn and winter (where the highest rates of the year are further increasing in land scenarios).

When additionally considering observed historical rainfall (combined scenario), the hydrologic impact of 50 years of changes is even more evident (past: annual −19%, summer −27%, peak flow −45%). Future projections by the COSMO-CLM regional climate model show enhanced seasonality, with drier summers (−33% precipitation with −16% intensity) and wetter autumns (+13% with +30% intensity). The drier future climate projection negates many of the simulated impacts of future land use change, resulting in a moderate hydrologic response, most notable in summer flow (+9%) and winter peak flow (+10%).

However, the severe hydrologic impacts of anthropogenic land transformation should be well considered, particularly in a zone of a variable climate with uncertain future direction. This requires adaptation in water management, which contrasted by the current land use trends. The urgency of these findings is not limited to the Mira catchment or the vast Italian *pianura padana*. Instead, the presented rural land transformation and hydrologic impacts are a common challenge in the lowland floodplains and deltas covering 22% of the global land surface and hosting our anthropogenic centres.

Conflict of interest

None.

Acknowledgements

This work would not have been possible without the expert knowledge and observational records by the local water management authority Consorzio di Bonifica Acque Risorgive. Special thanks goes out to ing. M. Cerni, ing. L. Mason and pumping manager G. Frison for their extended efforts and cooperation. We also thank the Environmental Protection Agency of Veneto (ARPAV) for providing meteorological data. The authors finally wish to thank the Editors and the three anonymous reviewers for their constructive comments and crucial insights, which helped to improve the manuscript.

References

ARPAV, 2016. Meteorological observations as conducted on a daily scale by the Agenzia Regionale per la Prevenzione e Protezione Ambientale del Veneto (ARPAV). (dataset).

Bakker, A., Bessembinder, J., 2012. Time Series Transformation Tool: Description of the Program to Generate Time Series Consistent with the KNMI '06 Climate Scenarios. .

Baruffi, F., Cisotto, A., Cimolino, A., Ferri, M., Monego, M., Norbiato, D., Cappelletto, M., Bisaglia, M., Pretner, A., Galli, A., Scarinci, A., Marsala, V., Panelli, C., Gualdi, S., Bucchignani, E., Torresan, S., Pasini, S., Critto, A., Marcomini, A., 2012. Climate change impact assessment on Veneto and Friuli plain groundwater. Part I: an integrated modeling approach for hazard scenario construction. Sci. Total Environ. 440, 154–166. doi:http://dx.doi.org/10.1016/j.scitotenv.2012.07.070.

Boling, A.A., Bouman, B.A.M., Tuong, T.P., Murty, M.V.R., Jatmiko, S.Y., 2007. Modelling the effect of groundwater depth on yield-increasing interventions in rainfed lowland rice in Central Java, Indonesia. Agric. Syst. 92, 115–139. doi:http://dx.doi.org/10.1016/j.agsy.2006.05.003.

Bozzola, M., Swanson, T., 2014. Policy implications of climate variability on agriculture: water management in the Po river basin, Italy. Environ. Sci. Policy 43, 26–38. doi:http://dx.doi.org/10.1016/j.envsci.2013.12.002.

Brauer, C.C., Teuling, A.J., Torfs, P.J.J.F., Uijlenhoet, R., 2014a. The Wageningen Lowland Runoff Simulator (WALRUS): a lumped rainfall-runoff model for catchments with shallow groundwater. Geosci. Model Dev. 7, 2313–2332. doi:http://dx.doi.org/10.5194/gmd-7-2313-2014.

Brauer, C.C., Torfs, P.J.J.F., Teuling, A.J., Uijlenhoet, R., 2014b. The Wageningen Lowland Runoff Simulator (WALRUS): Application to the Hupsel Barook catchment and the Cabauw polder. Hydrol. Earth Syst. Sci. 18, 4007–4028. doi:http://dx.doi.org/10.5194/hess-18-4007-2014.

Brauer, C.C., Overeem, A., Leijnse, H., Uijlenhoet, R., 2016. The effect of differences between rainfall measurement techniques on groundwater and discharge simulations in a lowland catchment. Hydrol. Process. 30, 3885–3900. doi:http://dx.doi.org/10.1002/hyp.10898.

Brown, A.G., Tooth, S., Bullard, J.E., Thomas, D.S.G., Chiverrell, R.C., Plater, A.J., Murton, J., Thorndycraft, V.R., Tarolli, P., Rose, J., Wainwright, J., Downs, P., Aalto, R., 2017. The geomorphology of the Anthropocene: emergence, status and implications. Earth Surf. Process. Landforms 42, 71–90. doi:http://dx.doi.org/10.1002/esp.3943.

Bucchignani, E., Montesarchio, M., Zollo, A.L., Mercogliano, P., 2016. High-resolution climate simulations with COSMO-CLM over Italy: Performance evaluation and climate projections for the 21st century. Int. J. Climatol. 36, 735–756. doi:http://dx.doi.org/10.1002/joc.4379.

Cazorzi, F., Dalla Fontana, G., De Luca, A., Sofia, G., Tarolli, P., 2013. Drainage network detection and assesment of network storage capacity in agrarion landscape. Hydrol. Process. 27, 541–553. doi:http://dx.doi.org/10.1002/hyp.9224.

Chin, A., 2006. Urban transformation of river landscapes in a global context. Geomorphology 79, 460–487. doi:http://dx.doi.org/10.1016/j.geomorph.2006.06.033.

Consorzio; di Bonifica Acque Risorgive, 2016. Unpublished data from the land reclamation consortium of basin Acque Risorgive [dataset].

Coppola, E., Giorgi, F., 2010. An assessment of temperature and precipitation change projections over Italy from recent global and regional climate model simulations. Int. J. Climatol. 30, 11–32. doi:http://dx.doi.org/10.1002/joc.1867.

Coppola, E., Verdecchia, M., Giorgi, F., Colaiuda, V., Tomassetti, B., Lombardi, A., 2014. Changing hydrological conditions in the Po basin under global warming. Sci. Total Environ. 493, 1183–1196. doi:http://dx.doi.org/10.1016/j.scitotenv.2014.03.003.

Crichton, D., 1999. The risk triangle. Nat. Disaster Manage. 102–103.

Dankers, R., Feyen, L., 2008. Climate change impact on flood hazard in Europe: an assessment based on high-resolution climate simulations. J. Geophys. Res. D Atmos. 113, D19105+. doi:http://dx.doi.org/10.1029/2007JD009719.

De Boer-Euser, T., Bouaziz, L., De Niel, J., Brauer, C., Dewals, B., Drogue, G., Fenicia, F., Grelier, B., Nossent, J., Pereira, F., Savenije, H., Thirel, G., Willems, P., 2017. Looking beyond general metrics for model comparison – Lessons from an international model intercomparison study. Hydrol. Earth Syst. Sci. 21, 423–440. doi:http://dx.doi.org/10.5194/hess-21-423-2017.

Desiato, F., Fioravanti, G., Fraschetti, P., Perconti, W., Piervitali, E., 2015. Il Clima Futuro in Italia: Analisi delle Proiezioni dei Modelli Regionali [italian]. Stato dell 'Ambiente 58 doi:http://dx.doi.org/10.1017/CBO9781107415324.004.
Ellis, E.C., 2011. Anthropogenic transformation of the terrestrial biosphere. Philos. Trans. R. Soc. A Math. Phys. Eng. Sci. 369, 1010–1035. doi:http://dx.doi.org/10.1098/rsta.2010.0331.
Fabian, L., 2012. Extreme cities and isotropic territories: scenarios and projects arising from the environmental emergency of the central Veneto città diffusa. Int. J. Disaster Risk Sci. 3, 11–22. doi:http://dx.doi.org/10.1007/s13753-012-0003-5.
Fan, Y., Li, H., Miguez-Macho, G., 2013. Global patterns of groundwater table depth. Science 339, 940–943. doi:http://dx.doi.org/10.1126/science.1229881.
Fatichi, S., Rimkus, S., Burlando, P., Bordoy, R., 2014. Does internal climate variability overwhelm climate change signals in streamflow? The upper Po and Rhone basin case studies. Sci. Total Environ. 493, 1171–1182. doi:http://dx.doi.org/10.1016/j.scitotenv.2013.12.014.
Giorgi, F., Lionello, P., 2008. Climate change projections for the Mediterranean region. Glob. Planet. Change 63, 90–104. doi:http://dx.doi.org/10.1016/j.gloplacha.2007.09.005.
Gupta, H.V., Kling, H., Yilmaz, K.K., Martinez, G.F., 2009. Decomposition of the mean squared error and NSE performance criteria: implications for improving hydrological modelling. J. Hydrol. 377, 80–91. doi:http://dx.doi.org/10.1016/j.jhydrol.2009.08.003.
IPCC, 2014. Climate Change 2014: Impacts, adaptation, and vulnerability. part B: regional aspects. Contribution of working group II to the Fifth Assessment Report of the Intergovernmental Panel on Climate Change, 688. Cambridge Univ. Press doi:http://dx.doi.org/10.1017/CBO9781107415324.004.
ISTAT, 2011. Il Futuro Demografico del Paese. (Municipality-level demographic data available in online data base from: http://dati.istat.it/ [dataset]).
IUAV, 2012. Catalogo delle foto aeree. (dataset).
Kennedy, J., Eberhart, R., 1995. Particle swarm optimization. Eng. Technol. 1942–1948. doi:http://dx.doi.org/10.1007/978-0-387-30164-8_630.
Kron, W., 2002. Keynote Lecture: Flood Risk = hazard X Exposure X Vulnerability. Flood Def..
Loos, R., 2015. Ontwikkeling van WALRUS-modellen voor FEWS Vecht. Internal report. Water board Vechtstromen, The Netherlands (dutch).
Marquardt, D.W., 1963. An algorithm for least-squares estimation of nonlinear parameters. J. Soc. Ind. Appl. Math. 11, 431–441. doi:http://dx.doi.org/10.1137/0111030.
Melsen, L.A., Addor, N., Mizukami, N., Newman, A.J., Torfs, P.J.J.F., Clark, M.P., Uijlenhoet, R., Teuling, A.J., 2018. Mapping (dis) agreement in hydrologic projections. Hydrol. Earth Syst. Sci. 22, 1775–1791. doi:http://dx.doi.org/10.5194/hess-22-1775-2018.
Milano, M., 2010. The foreseeable impacts of climate change on the water resources of four major Mediterranean catchment basins. Plan Blue – Reg. Act. Cent. (Sophia Antipolis) 1–8.
Milelli, M., Oberto, E., Parodi, A., 2008. Severe rainfall event in north-western Italy: 17 August 2006. Adv. Sci. Res. 2, 133–138. doi:http://dx.doi.org/10.5194/asr-2-133-2008.
Nash, J.E., Sutcliffe, J.V., 1970. River flow forecasting through conceptual models part I-a discussion of principles*. J. Hydrol. 10, 282–290. doi:http://dx.doi.org/10.1016/0022-1694(70)90255-6.
Nature editorial, 2003. Welcome to the Anthropocene. Nature 424 (709), 424. doi:http://dx.doi.org/10.1038/424709b.
Navarra, A., Tubiana, L., 2013. Regional assessment of climate change in the Mediterranean. Springer doi:http://dx.doi.org/10.1007/978-94-007-5781-3.
Pistocchi, A., Calzolari, C., Malucelli, F., Ungaro, F., 2015. Soil sealing and flood risks in the plains of Emilia-Romagna, Italy. J. Hydrol. Reg. Stud. 4, 398–409. doi:http://dx.doi.org/10.1016/j.ejrh.2015.06.021.
Poff, N.L.R., Bledsoe, B.P., Cuhaciyan, C.O., 2006. Hydrologic variation with land use across the contiguous United States: geomorphic and ecological consequences for stream ecosystems. Geomorphology 79, 264–285. doi:http://dx.doi.org/10.1016/j.geomorph.2006.06.032.
Ranzato, M., 2011. Integrated water design for a decentralized urban landscape: The case of the lowlands of the Veneto città diffusa. University of Trento (Ph.D. thesis).
Regione Veneto, 2007. Corine Land Classification inventory. (dataset).
Regione Veneto, 2011a. Demographic Inventory of the Veneto region between 1971-2011 at level of municipality. (dataset).
Regione Veneto, 2011b. Regional Soil Sampling Inventory Conducted by ARPAV. (italian] [dataset).
Regione Veneto, 2016. Piezometric Groundwater Measurements Per Season, Conducted by ARPAV. (dataset).
Rockel, B., Will, A., Hense, A., 2008. The regional climate model COSMO-CLM (CCLM). Meteorol. Zeitschrift 17, 347–348. doi:http://dx.doi.org/10.1127/0941-2948/2008/0309.
Santini, M., Valentini, R., 2011. Predicting hot-spots of land use changes in Italy by ensemble forecasting. Reg. Environ. Change 11, 483–502. doi:http://dx.doi.org/10.1007/s10113-010-0157-x.
Sheffield, J., Wood, E.F., Roderick, M.L., 2012. Little change in global drought over the past 60 years. Nature 491, 435–438. doi:http://dx.doi.org/10.1038/nature11575.
Slenters, V., 2014. WALRUS en WINFO: het simuleren van afvoeren voor een nieuw voorwaarschuwingssysteem, MSc internship report, Wageningen, The Netherlands. (dutch).
Smith, R.G.A., Pereira, L.S., Raes, D., Smith, M., 1998. Irrigation and Drainage Paper 56. FAO, pp. 97–156. doi:http://dx.doi.org/10.1061/(ASCE)0733-9437(2005)131:1(2).
Sofia, G., Tarolli, P., 2017. Hydrological response to ∼30 years of agricultural surface water management. Land 6, 3. doi:http://dx.doi.org/10.3390/land6010003.
Sofia, G., Prosdocimi, M., Dalla Fontana, G., Tarolli, P., 2014. Modification of artificial drainage networks during the past half-century: evidence and effects in a reclamation area in the Veneto floodplain (Italy). Anthropocene 6, 48–62. doi:http://dx.doi.org/10.1016/j.ancene.2014.06.005.
Sofia, G., Roder, G., Dalla Fontana, G., Tarolli, P., 2017. Flood dynamics in urbanised landscapes: 100 years of climate and humans' interaction. Sci. Rep. 7, 40527. doi:http://dx.doi.org/10.1038/srep40527.
Tarolli, P., Sofia, G., 2016. Human topographic signatures and derived geomorphic processes across landscapes. Geomorphology 255, 140–161. doi:http://dx.doi.org/10.1016/j.geomorph.2015.12.007.
Thomson, A.M., Calvin, K.V., Smith, S.J., Kyle, G.P., Volke, A., Patel, P., Delgado-Arias, S., Bond-Lamberty, B., Wise, M.A., Clarke, L.E., Edmonds, J.A., 2011. RCP4.5: a pathway for stabilization of radiative forcing by 2100. Clim. Change 109, 77–94. doi:http://dx.doi.org/10.1007/s10584-011-0151-4.
Van Loon, A.F., Stahl, K., Di Baldassarre, G., Clark, J., Rangecroft, S., Wanders, N., Gleeson, T., Van Dijk, A.I.J.M., Tallaksen, L.M., Hannaford, J., Uijlenhoet, R., Teuling, A.J., Hannah, D.M., Sheffield, J., Svoboda, M., Verbeiren, B., Wagener, T., Van Lanen, H.A.J., 2016. Drought in a human-modified world: reframing drought definitions, understanding, and analysis approaches. Hydrol. Earth Syst. Sci. 20, 3631–3650. doi:http://dx.doi.org/10.5194/hess-20-3631-2016.
Vautard, R., Gobiet, A., Jacob, D., Belda, M., Colette, A., Déqué, M., Fernández, J., García-Díez, M., Goergen, K., Güttler, I., Halenka, T., Karacostas, T., Katragkou, E., Keuler, K., Kotlarski, S., Mayer, S., van Meijgaard, E., Nikulin, G., Patarčić, M., Scinocca, J., Sobolowski, S., Suklitsch, M., Teichmann, C., Warrach-Sagi, K., Wulfmeyer, V., Yiou, P., 2013. The simulation of European heat waves from an ensemble of regional climate models within the EURO-CORDEX project. Clim. Dyn. 41, 2555–2575. doi:http://dx.doi.org/10.1007/s00382-013-1714-z.
Vaz, E., Nijkamp, P., 2015. Gravitational forces in the spatial impacts of urban sprawl: an investigation of the region of Veneto, Italy. Habitat Int. 45, 99–105. doi:http://dx.doi.org/10.1016/j.habitatint.2014.06.024.
Vezzoli, R., Mercogliano, P., Pecora, S., Zollo, A.L., Cacciamani, C., 2015. Hydrological simulation of po river (North Italy) discharge under climate change scenarios using the RCM COSMO-CLM. Sci. Total Environ. 521–522, 346–358. doi:http://dx.doi.org/10.1016/j.scitotenv.2015.03.096.
Yan, R., Gao, J., Huang, J., 2016. WALRUS-paddy model for simulating the hydrological processes of lowland polders with paddy fields and pumping stations. Agric. Water Manage. doi:http://dx.doi.org/10.1016/j.agwat.2016.02.018.
Zalasiewicz, J., Williams, M., Smith, A., Barry, T.L., Coe, A.L., Bown, P.R., Brenchley, P., Cantrill, D., Gale, A., Gibbard, P., Gregory, F.J., Hounslow, M.W., Kerr, A.C., Pearson, P., Knox, R., Powell, J., Waters, C., Marshall, J., Oates, M., Rawson, P., Stone, P., 2008. Are we now living in the Anthropocene. GSA Today 18, 4. doi:http://dx.doi.org/10.1130/GSAT01802A.1.
Zalasiewicz, J., Williams, M., Haywood, A., Ellis, M., 2011. The Anthropocene: a new epoch of geological time? Philos. Trans. R. Soc. A Math. Phys. Eng. Sci. 369, 835–841. doi:http://dx.doi.org/10.1098/rsta.2010.0339.
Zambrano-Bigiarini, M., Rojas, R., 2013. A model-independent Particle Swarm Optimisation software for model calibration. Environ. Modell. Softw. 43, 5–25. doi:http://dx.doi.org/10.1016/j.envsoft.2013.01.004.
Zollo, A.L., Rillo, V., Bucchignani, E., Montesarchio, M., Mercogliano, P., 2016. Extreme temperature and precipitation events over Italy: assessment of high-resolution simulations with COSMO-CLM and future scenarios. Int. J. Climatol. 36, 987–1004. doi:http://dx.doi.org/10.1002/joc.4401.